

Quark Model Study of Doubly Heavy Ξ and Ω Baryons via Deep Neural Network and Hybrid Optimization

Zahra Ghalenovi^{1*}, Masoumeh Moazzen Sorkhi¹ and Amir Hossein Sovizi²

¹Department of Physics, Kosar University of Bojnord, Bojnourd 94156-15458, Iran

²Yadegar Emam, Shahre Rey Branch, Islamic Azad University, Tehran 18155-144, Iran

Abstract

In the present work we investigate the mass spectrum and semileptonic decays of double charm and bottom baryon states using the hypercentral quark model. We solve the six-dimensional Schrödinger equation via deep learning and particle swarm optimization techniques to improve the speed and accuracy. Then, we predict the masses of the ground and excited states of single and doubly heavy baryons. Working close to the zero recoil point, we also study the semileptonic decay widths and branching ratios of doubly heavy Ξ and Ω baryons for the $b \rightarrow c$ transitions. A comparison between our results and the evaluations of other theoretical models is also presented. Our predictions of mass spectrum and decay widths provide valuable information for the experiment searching for undiscovered heavy baryon states.

1 Introduction

During the last few years various theoretical models have been presented on heavy baryon spectroscopy and study on this topic has been of special interest [1, 2, 3]. For the singly heavy baryons, mass spectra and some semileptonic decays have been measured in experiments [4, 5, 6, 7, 8, 9, 10, 11, 12, 13]. In 2002 the SELEX Collaboration reported the first observation of $M_{\Xi_{cc}^{++}} = 3518 \pm 1.7$ MeV [14] for doubly heavy Ξ_{cc}^{++} baryon state. Later, the new data has been reported by the LHCb Collaboration [15, 16]. Recently, the LHCb collaboration has started new searches on the Ξ_{bc} and Ω_{bc} doubly heavy baryons, but these baryon states are not yet to be observed [17, 18, 19]. In comparison to the doubly charmed Ξ_{cc} baryon, searching for the other doubly heavy states are more complicated. The search for these states is really hard for the experiment since higher energy and higher beam luminosity are required to produce them. For the semileptonic decay widths of doubly heavy baryons there are also a limited number of calculations reported by theoretical studies [20, 21, 22, 23, 24, 25, 26, 26, 27, 28, 29] and proposing a theoretical model on this topic is of great interest.

In recent years, machine learning has been the most popular computational approach for different fields of modern science and a significant raise of interest has been seen in that area. The machine learning techniques enable us to improve the performance and accuracy in theory and experiment.

The solution of three-body Schrödinger equation is a complicated problem in hadron physics. The machine learning techniques such as deep neural network (DNN) help us to solve this problem in a short time. Deep learning algorithms can identify the energy eigenvalues of the baryon systems [34, 35, 30]. In this study, we present a mathematical model using the DNN combining with particle swarm optimization algorithm (PSO) which is fast and provides high accuracy in mass estimation of the single and doubly heavy baryons. Some earlier works studied the heavy hadron properties via neural networks and deep learning techniques [30, 31, 32, 33]. Ref. [30] solved the nonrelativistic Schrödinger

*z_ghalenovi@kub.ac.ir

equation via neural networks and calculated the masses of the heavy Ω_b baryon states in a hypercentral approach. Ref. [31] used the neural networks and Gaussian processes to calculate the mass spectra of the light baryons, heavy charm mesons and pentaquark states. The authors of Ref. [32] presented two approaches using the deep neural networks to study the masses and decay widths of the mesons. Ref. [33] solved five-body Schrödinger equation of pentaquark states by using the neural networks and predicted the parities of these states.

In the present work, the single and doubly heavy baryon states are studied in a quark model. Firstly, we introduce our model and simplify the six-dimensional Schrödinger equation using the hypercentral model. Then, by applying the deep learning techniques, we evaluate the energy eigenvalues of the considered baryon system. In our method, we also use the particle swarm optimization to get the best values of the energies. In the next step, we predict the mass spectra of the ground and excited states of the single and doubly heavy baryons and present a comparison between our results and the experimental measurements or other theoretical predictions. The exist experimental data of the single heavy baryon masses help us to optimize our mass evaluations of the Ξ and Ω doubly heavy baryons. Finally, we simplify the form factors of $b \rightarrow c$ semileptonic decays and evaluate the semileptonic decay widths and branching ratios of the doubly heavy Ξ and Ω baryons. It helps us to get a deep understanding of their structure.

The structure of the present work is as follows. In Section 2 we introduce the three-body hypercentral quark model and present our potential model. In Section 3 the deep neural networks is briefly introduced. Our calculations of the single and doubly heavy baryon masses are presented in Section 5. In Section 6 we simplify the form factors of the considered transitions and calculate the semileptonic decay widths and corresponding branching fractions of doubly charm and bottom heavy baryons. A short summary is given in Section 7.

2 Phenomenological model

In the heavy-quark sector of heavy baryons one can use a non-relativistic formalism to study these states. The configurations of three quarks of baryons can be described by the Jacobi coordinates, ρ and λ ,

$$\vec{\rho} = \frac{1}{\sqrt{2}}(\vec{r}_1 - \vec{r}_2), \quad \vec{\lambda} = \frac{1}{\sqrt{6}}(\vec{r}_1 + \vec{r}_2 - 2\vec{r}_3) \quad (1)$$

such that

$$m_\rho = \frac{2m_1m_2}{m_1 + m_2}, \quad m_\lambda = \frac{2m_3(m_1^2 + m_2^2 + m_1m_2)}{(m_1 + m_2)(m_1 + m_2 + m_3)} \quad (2)$$

Here m_1 , m_2 and m_3 are the constituent quark masses. In the hypercentral model, the hyperradius x and hyperangle ζ are given in terms of the Jacobi coordinates ρ and λ [36, 37] by

$$x = \sqrt{\rho^2 + \lambda^2}, \quad \xi = \arctan\left(\sqrt{\frac{\rho}{\lambda}}\right). \quad (3)$$

The Hamiltonian of the baryon system takes the form

$$H = \frac{p_\rho^2}{2m_\rho} + \frac{p_\lambda^2}{2m_\lambda} + V(x). \quad (4)$$

The hyperradial baryon wave function $\psi_{\nu,\gamma}(x)$ is defined as a solution of the following equation (for details see Refs. [37, 41])

$$\left[\frac{d^2}{dx^2} + \frac{5}{x} \frac{d}{dx} - \frac{\gamma(\gamma+4)}{x^2}\right]\psi_{\nu,\gamma}(x) = -2m[E_{\nu,\gamma} - V(x)]\psi_{\nu,\gamma}(x). \quad (5)$$

where m is the reduced mass and γ is the grand angular quantum number. ν counts the nodes of the wave function. We consider the Killingbeck potential given by [41]

$$V(x) = \alpha x^2 + \beta x - \frac{\tau}{x}, \quad (6)$$

here, x is the hyperradius and α , β and τ are constant. In the present work, we solve the Schrödinger equation 5 using deep learning technique combined with a PSO algorithm. We use a trial wave function as proposed in our previous works [38, 39]. In the present study we consider the baryon states with zero nodes $\nu = 0$, and neglect the spin dependent interactions.

3 Deep Learning Model for Energy Evaluation

The first step in our framework involves the generation of a synthetic dataset by solving the Schrödinger equation and using the shooting method. The Schrödinger equation for the system under study is expressed as

$$\left[\frac{d^2}{dx^2} + \frac{5}{x} \frac{d}{dx} - \frac{\gamma(\gamma+4)}{x^2} - 2m\alpha x^2 - 2m\beta x + \frac{2m\tau}{x} \right] \psi_\gamma(x) = -2mE_\gamma \psi_\gamma(x). \quad (7)$$

The goal is to compute E_γ energy eigenvalues such that the boundary conditions for $\psi_\gamma(x)$ are satisfied. In this step deep learning model is used to predict energy eigenvalues based on the features in dataset.

3.1 Model Architecture

The deep neural networks consist of three layers: an input layer, hidden layers, and output layer. In the present work, we employ a feed forward neural network with one input layer, two hidden layers and one output layer to solve the differential equation 7. The output layer consists of a single neuron to predict the E_γ energy eigenvalues.

3.2 Training Procedure

The neural network is trained using the mean squared error (MSE) loss function:

$$MSE = \frac{1}{n} \sum_{i=1}^n (Y_{\text{true}} - Y_{\text{pred}})^2, \quad (8)$$

where n , Y_{true} and Y_{pred} are the number of data points, actual value for i -th data point and predicted value for the i -th data point. We employ the adaptive moment estimation optimizer for adaptive learning rate adjustments during training. The model is trained over a large number of epochs to ensure convergence. The dataset is split into 80% training and 20% validation subsets. The root mean squared error (RMSE) and MSE show the validity of our model and its accuracy.

4 Particle Swarm Optimization (PSO)

For further refines of energy evaluations, we employ the particle swarm optimization. PSO is an effective method in finding global optima in multi-dimensional search spaces. A swarm of particles is initialized randomly, where each particle represents a solution (energy value). The position of each particle is updated iteratively, and the fitness of each particle is evaluated using the trained deep learning model. The fitness function for each particle is based on the difference between the predicted energy value and the target energy value. The goal is to minimize this difference. The global best solution found by PSO algorithm represents the optimal energy estimations.

5 Heavy baryon mass spectra

By using the obtained E_γ energies, one can evaluate the mass spectra of the baryon systems. The quark masses are taken from our previous work [38]. We consider $m_q=320$ MeV, $m_s=440$ MeV, $m_c=1600$ MeV and $m_b=4670$ MeV.

Table 1: Masses of the ground and excited states of single charm baryons (in GeV).

State	Baryon	Our results	Exp [40]	NRQM[41]	NRQM[43]
<i>S</i> -wave	Σ_c	2.453	2.455	2.459	2.452
	Ξ_c	2.463	2.465	2.504	2.473
	Ω_c	2.694	2.695	2.566	2.695
<i>P</i> -wave	Σ_c	2.791	2.792		2.794
	Ξ_c	2.789	2.791		2.726
	Ω_c	3.063	3.065		2.996
<i>D</i> -wave	Σ_c	3.088			3.058
	Ξ_c	3.113			2.960
	Ω_c	3.325			3.230

Table 2: Masses of the ground and excited states of single bottom baryons (in GeV).

State	Baryon	Our result	Exp [40]	NRQM[41]	NRQM[44]	RPH[45]
<i>S</i> -wave	Σ_b	5.808	5.810	5.808	5.816	5813
	Ξ_b	5.925	5.797	5.848	5.793	5.793
	Ω_b	6.043	6.045	5.903	6.048	6.048
<i>P</i> -wave	Σ_b	6.096	6.098		6.105	6.098
	Ξ_b	6.213	6.227		6.133	6.080
	Ω_b	6.337	6.339		6.321	6.325
<i>D</i> -wave	Σ_b	6.384			6.363	6.369
	Ξ_b	6.352			6.355	6.354
	Ω_b	6.631			6.554	6.590

We calculated the masses of the ground and *P*-wave and *D*-wave excited states of single and doubly heavy baryons and list them in Tables 1, 2, 3 and 4. We compare the obtained masses with the exist experimental data [40] and those of other theoretical models; non-relativistic quark model (NRQM), relativistic quark model (RQM), heavy diquark effective theory (EFT), heavy quark spin symmetry (HQSS) and Regge phenomenology (RPH) [41, 42, 43, 44, 45, 46, 47, 48, 49, 50, 51]. In our previous studies within a quark model we solved the Schrödinger equation by a numerical method and consider the heavy baryon states [41, 42]. Our mass evaluations of the single charm and bottom baryons are listed in Tables 1 and 2. Our results are in good agreement with the experimental masses. Our predictions for the ground and orbitally excited states of doubly heavy baryons are also summarized in Tables 3 and 4. We could obtain the experimental mass of the Ξ_{cc}^{++} doubly heavy baron [16] for the *qcc* baryon state in Table 3.

Table 3: Masses of ground states of double charm and bottom baryons (in GeV).

Baryon	Content	Our results	NRQM[42]	NRQM[46]	RQM[47]	NRQM[48]
Ξ_{cc}	qcc	3.620	3.679	3.613	3.676	3.685
Ξ_{bc}	qbc	7.050	7.003	6.928	7.020	
Ξ_{bb}	qbb	10.200	10.325	10.198	10.340	10.314
Ω_{cc}	scc	3.750	3.830	3.712	3.815	3.832
Ω_{bc}	sbc	6.900	7.149	7.013	7.147	
Ω_{bb}	sbb	10.400	10.466	10.269	10.456	10.447

Table 4: Masses of excited states of double charm and bottom baryons (in GeV).

State	Baryon	Our results	NRQM[49]	EFT[50]	NRQM[51]
P -wave	Ξ_{cc}	3.928	3.853	4.028	3.855
	Ξ_{bc}	7.266	7.140		
	Ξ_{bb}	10.631	10.502	10.386	10.417
	Ω_{cc}	4.106	3.964	4.086	4.002
	Ω_{bc}	7.4457	7.375		
	Ω_{bb}	10.808	10.634	10.607	10.560
D -wave	Ξ_{cc}	4.237	4.026	4.321	
	Ξ_{bc}	7.575	7.307		
	Ξ_{bb}	10.939	10.658	10.585	
	Ω_{cc}	4.414	4.133	4.263	
	Ω_{bc}	7.754	7.807		
	Ω_{bb}	11.1177	10.783	10.723	

6 Semileptonic decay widths of $B \rightarrow B'l\bar{\nu}$ transitions and branching fractions

The semileptonic decays caused by the weak force in which a new hadron, a lepton and a neutrino are produced. To consider the semileptonic decays one needs to determine the transition form factors. There are different methods to simplify the transition form factors [52, 54, 55, 56]. The methodology for the decay widths are similar to the pattern employed in our previous study [38].

The elements of the semileptonic transition matrix are defined by the weak hadronic and leptonic currents (J_μ and \mathcal{L}^μ)

$$T = \frac{G_F}{\sqrt{2}} V_{cb} J_\mu \mathcal{L}^\mu \quad (9)$$

where G_F and V_{bc} refers to the Fermi Coupling constant and CKM matrix element.

$$J_\mu = V_\mu - A_\mu = \bar{\psi}^c \gamma_\mu (I - \gamma_5) \psi^b, \quad \mathcal{L}^\mu = \bar{l} \gamma^\mu (1 - \gamma_5) \nu_l \quad (10)$$

where $\psi^{b(c)}$ is the charm or bottom quark field and $V_\mu \equiv \bar{\psi}^c \gamma_\mu \psi^b$ and $A_\mu \equiv \bar{\psi}^c \gamma_\mu \gamma_5 \psi^b$. The hadron matrix elements is given as follows

$$\begin{aligned} H_\mu &= \langle B'(p', s') | V_\mu - A_\mu | B(p, s) \rangle = \langle B'(p', s') | \bar{\psi}^c \gamma_\mu (I - \gamma_5) \psi^b | B(p, s) \rangle \\ &= \bar{u}'(p', s') \{ \gamma_\mu (F_1(\omega) - \gamma_5 G_1(\omega)) + v_\mu (F_2(\omega) - \gamma_5 G_2(\omega)) \\ &\quad + v'_\mu (F_3(\omega) - \gamma_5 G_3(\omega)) \} u(p, s) \end{aligned} \quad (11)$$

where $|B(p, s)\rangle$ and $|B'(p', s')\rangle$ refers to the initial and final baryons. $u(p, s)$ and $u'(p', s')$ are Dirac spinors, and $v_\mu = p_\mu/m_B$ ($v'_\mu = p'_\mu/m'_{B'}$) is the four velocity of the corresponding baryon. $F_i(\omega)$ and $G_i(\omega)$ refer to the form factors. The differential decay rates are given by

$$\frac{d\Gamma}{d\omega} = \frac{d\Gamma_L}{d\omega} + \frac{d\Gamma_T}{d\omega}. \quad (12)$$

in which Γ_L and Γ_T are the longitudinally and transversely polarized W's respectively and obtained in terms of the transition form factors [26, 27]

$$\frac{d\Gamma_T}{d\omega} = \frac{G_F^2 |V_{cb}|^2 M_{B'}^3}{12\pi^3} \sqrt{\omega^2 - 1} q^2 \{(\omega - 1)|F_1(\omega)|^2 + (\omega + 1)|G_1(\omega)|^2\}, \quad (13)$$

and

$$\frac{d\Gamma_L}{d\omega} = \frac{G_F^2 |V_{cb}|^2 M_{B'}^3}{24\pi^3} \sqrt{\omega^2 - 1} \{(\omega - 1)|\mathcal{F}^V(\omega)|^2 + (\omega + 1)|\mathcal{F}^A(\omega)|^2\}, \quad (14)$$

where

$$\begin{aligned} \mathcal{F}^{V,A}(\omega) &= \left[(m_B \pm m_{B'}) F_1^{V,A}(\omega) + (1 \pm \omega) \left(m_{B'} F_2^{V,A}(\omega) + m_B F_3^{V,A}(\omega) \right) \right], \\ F_j^V &\equiv F_j(\omega), \quad F_j^A \equiv G_j(\omega), \quad j = 1, 2, 3 \end{aligned} \quad (15)$$

where the lepton masses are neglected. The velocity transfer $\omega (= v \cdot v')$ takes the values between $\omega = 1$ to the maximum of $\omega_{max} = (m_B^2 + m_{B'}^2)/(2m_B m_{B'})$. The decay width is obtained as follows

$$\Gamma = \int_1^{\omega_{max}} d\omega \frac{d\Gamma}{d\omega} = \int_1^{\omega_{max}} d\omega \left(\frac{d\Gamma_L}{d\omega} + \frac{d\Gamma_T}{d\omega} \right). \quad (16)$$

Different studies have simplified the transition form factors of the semileptonic decays [52, 54, 55, 56]. Ref. [52] has simplified the form factors employing a Lorentz covariant quark model. In the heavy quark limit and near to zero recoil point, the weak form factors can be simplified and expressed by a single IW function $\eta(\omega)$ [52, 57, 58]

$$\begin{aligned} F_1(\omega) &= G_1(\omega) = \eta(\omega), \\ F_2(\omega) &= F_3(\omega) = G_2(\omega) = G_3(\omega) = 0. \end{aligned} \quad (17)$$

The universal function $\eta(\omega)$ is defined as [52]

$$\eta(\omega) = \exp\left(-3(\omega - 1)\frac{m_{bb}^2}{\Lambda_B^2}\right) \quad (18)$$

where $m_{bb} = 2m_b$ for the $bb \rightarrow bc$ transitions. Λ_B depends on the size of a baryon and ranges from $2.5 \leq \Lambda_B \leq 3.5$ GeV [52] where, the smaller of Λ_B gives smaller decay widths. In the case of the $bc \rightarrow cc$ transitions, m_{bb} should be replaced by m_{cc} and therefore, the IW functions for $bb \rightarrow bc$ and $bc \rightarrow cc$ transitions depends on the heavy flavor factors. The Λ_B dependence of η functions for $\Omega_{bb} \rightarrow \Omega_{bc}$ and $\Xi_{bb} \rightarrow \Xi_{bc}$ transitions (with $\Lambda_B = 2.5$ GeV and $\omega = \omega_{max}$) is plotted in Fig. 1.

The ω dependence of the semileptonic decay rates of $\Xi_{bb} \rightarrow \Xi_{bc} \ell \bar{\nu}_\ell$, and $\Xi_{bc} \rightarrow \Xi_{cc} \ell \bar{\nu}_\ell$ transitions is shown in Figs. 2 and 3 respectively.

Regarding the equation 17 one can get the following relations

$$\frac{d\Gamma_T}{d\omega} = \frac{G_F^2 |V_{cb}|^2 M_{B'}^3}{6\pi^3} q^2 \omega \sqrt{\omega^2 - 1} \eta^2(\omega), \quad (19)$$

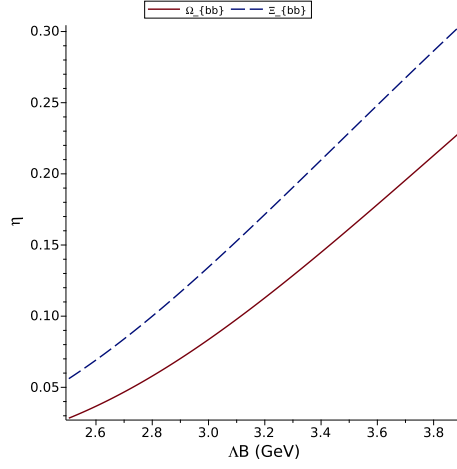


Figure 1: η function versus Λ_B for $\Omega_{bb} \rightarrow \Omega_{bc} \ell \bar{\nu}_\ell$ and $\Xi_{bb} \rightarrow \Xi_{bc} \ell \bar{\nu}_\ell$ transitions ($\ell = e$ or μ).

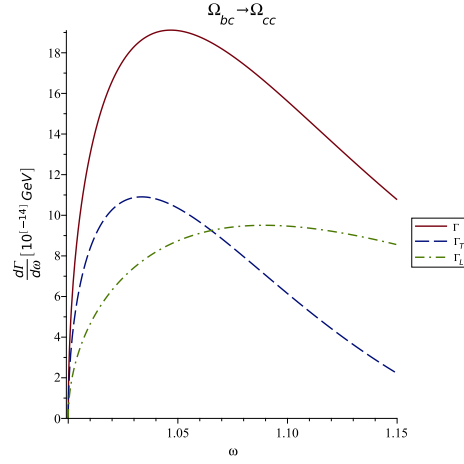


Figure 2: $\frac{d\Gamma_T}{d\omega}$, $\frac{d\Gamma_L}{d\omega}$ and $\frac{d\Gamma}{d\omega}$ semileptonic decay widths for $\Xi_{bc} \rightarrow \Xi_{cc} \ell \bar{\nu}_\ell$ transition ($\ell = e$ or μ).

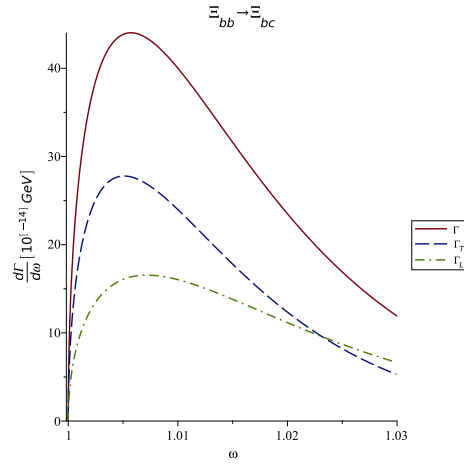


Figure 3: $\frac{d\Gamma_T}{d\omega}$, $\frac{d\Gamma_L}{d\omega}$ and $\frac{d\Gamma}{d\omega}$ semileptonic decay widths for $\Xi_{bb} \rightarrow \Xi_{bc} \ell \bar{\nu}_\ell$ transition ($\ell = e$ or μ).

Table 5: Semileptonic decay widths of double charm and bottom baryons (in units of 10^{-14} GeV).

Decay	Our results	NRQM[38]	RCQM [52]	NRQM [53]	HQSS [24]	LFQM ¹ [28]
$\Xi_{bc} \rightarrow \Xi_{cc}\ell\bar{\nu}_\ell$	$4.47^{+1.0}_{-1.20}$	4.39 ± 0.83	4.01 ± 1.21	5.07	$2.57^{+0.26}_{-0.03}$	4.50
$\Xi_{bb} \rightarrow \Xi_{bc}\ell\bar{\nu}_\ell$	$1.66^{+0.73}_{-0.64}$	1.75 ± 0.73	1.33 ± 0.61	1.63	$1.92^{+0.25}_{-0.05}$	3.30
$\Omega_{bc} \rightarrow \Omega_{cc}\ell\bar{\nu}_\ell$	$3.55^{+0.67}_{-0.84}$	4.70 ± 0.83	4.12 ± 1.10	5.39	$2.59^{+0.20}$	3.94
$\Omega_{bb} \rightarrow \Omega_{bc}\ell\bar{\nu}_\ell$	$2.01^{+0.99}_{-0.80}$	1.87 ± 0.76	1.92 ± 1.15	2.48	$2.14^{+0.20}_{-0.02}$	3.69

The branching ratios can be obtained as following

$$\mathcal{B} = \Gamma \times \tau, \quad (20)$$

where τ is the lifetime of the initial baryon. We take the values of $\tau_{\Xi_{bb}} = 370 \times 10^{-15}s$, $\tau_{\Xi_{bc}} = 244 \times 10^{-15}s$ [59], $\tau_{\Omega_{bc}} = 220 \times 10^{-15}s$, and $\tau_{\Omega_{bb}} = 800 \times 10^{-15}s$ [60, 61] to evaluate the branching fractions.

Table 6: The calculated branching ratios of semileptonic decays of double charm and bottom baryons.

Process	Our results	NRQM [38]	NRQM [53]	LFQM [28]
$\Xi_{bc} \rightarrow \Xi_{cc}\ell\bar{\nu}_\ell$	1.65×10^{-2}	1.63×10^{-2}	1.11×10^{-2}	1.67×10^{-2}
$\Xi_{bb} \rightarrow \Xi_{bc}\ell\bar{\nu}_\ell$	0.61×10^{-2}	0.98×10^{-2}	0.28×10^{-2}	1.86×10^{-2}
$\Omega_{bc} \rightarrow \Omega_{cc}\ell\bar{\nu}_\ell$	1.18×10^{-2}	1.57×10^{-2}	1.10×10^{-2}	1.32×10^{-2}
$\Omega_{bb} \rightarrow \Omega_{bc}\ell\bar{\nu}_\ell$	2.45×10^{-2}	2.27×10^{-2}		4.49×10^{-2}

The evaluated semileptonic decay widths of doubly heavy baryons are listed in Table 5. We take $\Lambda_B = 3$. The uncertainties in our predicted widths are due to the parameter Λ_B , which varies in the range of 2.5 – 3.5 GeV. We compare our results with those evaluated by other theoretical works [24, 28, 38, 52, 53]. Our predicted decay widths are close to the ones obtained by Ref. [52]. For the $\Xi_{bc} \rightarrow \Xi_{cc}$, $\Xi_{bb} \rightarrow \Xi_{bc}$ and $\Omega_{bb} \rightarrow \Omega_{bc}$ transitions, our results are also in good agreement with those of our previous work [38]. The evaluated branching fractions of semileptonic decays are summarized in Table 6 and compared with other evaluations [28, 38, 53]. We hope our results are helpful to find the value of the CKM matrix element V_{cb} from next experiments.

7 Summary

In the present work, we propose our phenomenological approach for estimation of energy eigenvalues of three-body baryon systems by integrating the deep learning with particle swarm optimization methods. By integrating deep learning with PSO, we could develop a powerful methodology for accurate energy prediction of three-body quantum systems. The deep learning model, trained on a large dataset generated using the shooting method, provides an initial estimate of the energy values while, PSO refines these predictions and leads to highly accuracy in calculations. This hybrid approach demonstrates the potential of combining machine learning and optimization techniques in solving challenging math problems in computational physics. By evaluation of baryon energies, we are able to predict the mass spectrum of the single and doubly heavy baryons which are not yet determined by experiment. The validity of our scheme for heavy baryon systems will be determined by consistency with the exist experimental data. Our evaluated masses are in a good agreement with the experiments and also with the predictions of other theoretical works. In our study the overall MSE, training MSE and validation

MSE are 6.443×10^{-5} , 6.690×10^{-5} and 6.196×10^{-5} respectively. We also study the semileptonic decays of doubly heavy Ξ and Ω baryons. We introduce a new form of the IW function, and evaluate the semileptonic decay widths and branching ratios of the $bb \rightarrow bc$ and $bc \rightarrow cc$ transitions. A comparison between our theoretical results and other available predictions shows our obtained results are acceptable. Our predictions will be able to guide the future searches for the undiscovered single and doubly heavy baryons at LHCb, ATLAS, and CMS.

References

- [1] X. Z. Weng, X. L. Chen, and W. Z. Deng, Phys. Rev. D **97**, 054008 (2018).
- [2] Z. Shah and A. K. Rai, Eur. Phys. J. C **77**, 129 (2017).
- [3] H. Garcilazo, A. Valcarce, and J. Vijande, Phys. Rev. D **94**, 074003 (2016).
- [4] S. Navas et al. (Particle Data Group), Phys. Rev. D **110**, 030001 (2024).
- [5] R. Aaij et al. [LHCb Collaboration], Phys. Rev. Lett. **118**, 182001 (2017).
- [6] J. Yelton et al. [Belle Collaboration], Phys. Rev. D **97**, 051102 (2018).
- [7] B. Aubert et al. [BaBar Collaboration], Phys. Rev. D **78**, 112003 (2008).
- [8] E. Solovieva et al. [Belle Collaboration], Phys. Lett. B **672**, Phys. Lett B **672**, 1-5 (2009).
- [9] M. Ablikim *et al.* (BESIII Collaboration), Phys. Lett. B **767**, 42 (2017).
- [10] M. Ablikim *et al.* (BESIII Collaboration), Phys. Rev. Lett. **121**, 251801 (2018).
- [11] Y. B. Li *et al.* (Belle Collaboration), Phys. Rev. Lett. **127**, 121803 (2021).
- [12] Y. B. Li *et al.* (Belle Collaboration), Phys. Rev. D **105**, L091101 (2022).
- [13] R. Ammar *et al.* (CLEO Collaboration), Phys. Rev. Lett. **89**, 171803 (2002).
- [14] M. Mattson *et al.* (SELEX Collaboration), Phys. Rev. Lett. **89**, 112001 (2002).
- [15] R. Aaij *et al.* (LHCb Collaboration), Phys. Rev. Lett. **119**, 112001 (2017).
- [16] R. Aaij *et al.* (LHCb Collaboration), Phys. Rev. Lett. **121**, 162002 (2018).
- [17] R. Aaij *et al.* (LHCb Collaboration), JHEP **11**, 095 (2020).
- [18] R. Aaij *et al.* (LHCb Collaboration), Chin. Phys. C **45**, 093002 (2021).
- [19] R. Aaij *et al.* (LHCb Collaboration), Chin. Phys. C **47**, 093001 (2023).
- [20] Zhen-Yu Li, Guo-Liang Yu, Zhi-Gang Wang, Jian-Zhong Gu, and Hong-Tao Shen, Mod. Phys. Lett. A **38**, 2350051 (2023).
- [21] Y. J. Shi, W. Wang and Z. X. Zhao, Eur. Phys. J. C **80**, 398 (2020).
- [22] T. Gutsche, A. Mikhail, M.A. Ivanov, J. G. Körner, V. E. Lyubovitskij and Z. Tyulemissov, Phys. Rev. D **100**, 114037 (2019).
- [23] Q.X. Yu, X.H. Guo, Nucl. Phys. B **947**, 114727 (2019).
- [24] E. Hernandez, J. Nieves and J. M. Verde-Velasco, Phys. Lett. B **663**, 234 (2008).

- [25] V. E. Lyubovitskij, A. Faessler, T. Gutsche, M. A. Ivanov, and J. G. Körner, *Prog. Part. Nucl. Phys.* **50**, 329 (2003).
- [26] C. Albertus, E. Hernandez and J. Nieves, *Phys. Rev. D* **71**, 014012 (2005).
- [27] C. Albertus, E. Hernandez, J. Nieves and J. M. Verde-Velasco, *Eur. Phys. J. A* **32**, 183 (2007), [Erratum]: *Eur. Phys. J. A* **36**, 119 (2008).
- [28] W. Wang, F. S. Yu, Z.X. Zhao, *Eur. Phys. J. C* **77**, 781 (2017).
- [29] Q. Qin, Y. J. Shi, W. Wang, Y. Guo-He, F. S. Yu and R. Zhu, *Phys. Rev. D* **103**, 3 (2022).
- [30] H. Mutuk, *Eur. Phys. J. A* **56**, 146 (2020).
- [31] Yarin Gal, Vishnu Jejjala, Damian Kaloni Mayorga Penac, Challenger, Mishraa, *Int. J. Mod. Phys. A* **37**, 2250031 (2022).
- [32] M. Malekhosseini, S. Rostami, A. R. Olamaei, R. Ostovar and K. Azizi, *Phys. Rev. D* **110**, 054011 (2024).
- [33] H. Mutuk, *Chin. Phys. C* **43**, 093103 (2019).
- [34] N. Yadav, A. Yadav, M. Kumar, *An Introduction to Neural Network Methods for Differential Equations*, Springer in Applied Sciences and Technology, (2015).
- [35] D. R. Parisi, M. C. Mariani, M. A. Laborde, *Chem. Eng. Process.* **42**, 715 (2003).
- [36] E. Santopinto, F. Iachello and M. M. Gainini, *Eur. Phys. J. A* **1**, 307 (1998);
- [37] M. M. Giannini, E. Santopinto and A. Vassallo, *Prog. Part. Nucl. Phys.* **50**, 263 (2003); *Eur. Phys. J. A* **12**, 447 (2001).
- [38] Z. Ghalenovi, C. P. Shen and M. Moazzen Sorkhi, *Phys. Lett. B* **834**, 137405 (2022).
- [39] Z. Ghalenovi and M. Moazzen Sorkhi, *Eur. Phys. J. Plus* **133**, 301 (2018).
- [40] S. Navas et al. (Particle Data Group), *Phys. Rev. D* **110**, 030001 (2024).
- [41] Z. Ghalenovi, A. A. Rajabi, S. X. Qin and D. H. Rischke, *Mod. Phys. Lett. A* **29**, 1450106 (2014).
- [42] Z. Ghalenovi and M. M. Sorkhi, *Chin. Phys. C* **47**, 3 (2023).
- [43] Z. Shah, K. Thakkar, A. Kumar Rai and P. C. Vinodkumar, *Eur. Phys. J. A* **52**, 313 (2016).
- [44] K. Thakkar, Z. Shah, A. Kumar Rai, P.C. Vinodkumar, *Nucl. Phys. A* **965**, 57 (2017).
- [45] Ke-Wei Wei, B. Chen, N. Liu, Q-Qian Wang, Xin-Heng Guo, *Phys. Rev. D* **95**, 116005 (2017).
- [46] C. Albertus, E. Hernández, and J. Nieves, *Phys. Lett. B* **683**, 21 (2010).
- [47] W. Roberts and M. Pervin, *Int. J. Mod. Phys. A* **23**, 2817 (2008).
- [48] T. Yoshida, E. Hiyama, A. Hosaka, M. Oka, and K. Sadato, *Phys. Rev. D* **92**, 114029 (2015).
- [49] Z. Shah, K. Thakkar and A. K. Rai, *Eur. Phys. J. C* **76**, 530 (2016).
- [50] J. Soto and J. T. Castellà, *Phys. Rev. D* **104**, 074027 (2021).
- [51] E. Ortiz-Pacheco and R. Bijker, *Phys. Rev. D* **108**, 054014 (2023).
- [52] A. Faessler, T. Gutsche, M. A. Ivanov, J. G. Körner, and V. E. Lyubovitskij, *Phys. Rev. D* **80**, 034025 (2009).

- [53] S. Rahmani, H. Hassanabadi, and H. Sobhani, *Eur. Phys. J. C* **80**, 312 (2020).
- [54] H. Georgi and M. B. Wise, *Phys. Lett. B* **243**, 279 (1990).
- [55] C. D. Carone, *Phys. Lett. B* **253**, 408 (1991).
- [56] J. M. Flynn and J. Neives, *Phys. Rev. D* **76**, 017502 (2007) [Erratum: *Phys. Rev. D* **77**, 099901 (2008)].
- [57] N. Isgur and M. B. Wise, *Nucl. Phys. B* **348**, 276 (1991).
- [58] D. Ebert, R. N. Faustov and V. O. Galkin, *Phys. Rev. D* **73**, 094002 (2006).
- [59] M. Karliner and J. L. Rosner, *Phys. Rev. D* **90**, 094007 (2014).
- [60] V. V. Kiselev and A. K. Likhoded, *Phys. Usp.* **172**, 497 (2002).
- [61] V. V. Kiselev and A. K. Likhoded, *Phys. Usp.* **45**, 455 (2002).